JOURNAL OF CATALYSIS 101, 262–267 (1986)

A Transmission Electron Microscope Study of the Effect of Cyclohexane Adsorption on the Crystallization of $Pd_{80}Si_{20}$ Metallic Glass

W. KOWBEL AND W. E. BROWER, JR.

Department of Mechanical Engineering and Energy Processes and Molecular Science Program, Southern Illinois University, Carbondale, Illinois 62901

Received August 28, 1985; revised April 18, 1986

The strong effect of the adsorption of cyclohexane on the crystallization of metastable $Pd_{80}Si_{20}$ metallic glass was studied *in situ* via a high voltage electron microscope equipped with a hot stage and an environmental cell. The crystallization temperature of the $Pd_{80}Si_{20}$ glass was lowered by 200°C in 20 Torr of cyclohexane as compared to 10^{-6} Torr vacuum. The path of the solid state phase transformation in the bulk glass was also altered, since a different crystalline second phase formed in cyclohexane as compared to vacuum.

INTRODUCTION

Amorphous $Pd_{80}Si_{20}$ flakes produced by the shock tube technique have been used as catalysts in hydrogenation and isomerization reactions of olefins (*1, 2*). Amorphous $Pd_{80}Si_{20}$ exhibits altered selectivity with respect to a crystalline Pd catalyst (*2*) and amorphous $Fe_{80}B_{20}$ exhibits high activity with respect to crystallized $Fe_{80}B_{20}$ (*3*). The Fischer–Tropsch reaction requires a temperature of 300–400°C, which is in the range of crystallization temperature for $Fe_{80}B_{20}$ glass in inert atmosphere and vacuum. Thus, knowledge of the kinetics of crystallization in both inert and reactive atmospheres is essential, if such nonequilibrium catalysts are to be maintained as glasses in hydrocarbon reactions.

It was reported by Masumoto and coworkers (*3*) that the crystallization temperature of $Fe_{80}B_{20}$ amorphous ribbon was lowered by 132°C during the Fischer–Tropsch reaction. They also observed up to a hundred times lower reaction rate after crystallization. It was found by Alp *et al.* (*4*) that the crystallization of $Fe_{80}B_{20}$ glass in the presence of inert gas differs from the crystallization in vacuum. Wagner (*5*) found a difference in the crystallization kinetics as a function of annealing atmosphere for $Fe_{78}Mo_2B_{20}$ metallic glass alloy. The crystallization temperature was higher in one atmosphere of argon as compared to 10^{-7} Torr vacuum.

Here we report the study of the crystallization of $Pd_{80}Si_{20}$ alloy glass in vacuum and in a cyclohexane atmosphere by using the high voltage electron microscope (HVEM) in conjunction with an *in situ* environmental cell available at Argonne National Laboratory.

EXPERIMENTAL PROCEDURE

The samples were prepared by using "shock tube" rapid solidification technique (*6*) from a master alloy of the composition $Pd_{80}Si_{20}$. The use of the HVEM at Argonne National Laboratory, which is equipped with 1.2-MeV accelerating voltage, enables the study of unthinned flakes produced by our shock tube splat cooler due to the useful depth of penetration of the electron beam of 1 μm. The resolution of the HVEM in the imaging mode is 3 Å. Using unthinned samples prevented spurious crystallization effects due to the electrolytic thinning process (*7*) and allows an evalua-

0021-9517/86 $3.00

FIG. 1. Stepwise aging procedure utilizing HVEM hot stage. Onset of crystallization in vacuum, Tc_1; onset of crystallization in cyclohexane, Tc_2.

tion of adsorption effects on the glassy surface which would be inserted into a reactor. The shock tube-produced flakes are nominally 5 μm thick, but have an irregular thickness with occasional holes. Large areas of the unthinned flakes are thin enough to become electron transparent at the high electron energies available in the HVEM. Two samples of $Pd_{80}Si_{20}$ were studied, one in normal TEM column vacuum of 10^{-6} Torr, and the second in the presence of 20 Torr cyclohexane. The first sample in the vacuum was heated in a stepwise procedure by successive 20-min isothermal treatments at 150, 300, 380, 400, 500, 600, and 630°C, shown schematically in Fig. 1. Heating to the next higher holding temperature took 1–2 min. The second sample was heated by the same procedure to 450°C. The difference between the two actual temperatures, 400 and 405°C (both nominally 400°C), arose from differences in resetting the hot stage power supply.

RESULTS

A. Vacuum Aging

The diffraction pattern and the image of the unaged $Pd_{80}Si_{20}$ sample in vacuum at room temperature are shown in Fig. 2. A low density of small crystallites can usually be detected in some sections of the as-quenched sample by imaging, but not by diffraction. The diffraction pattern showed only two diffuse bands indicating an ini-

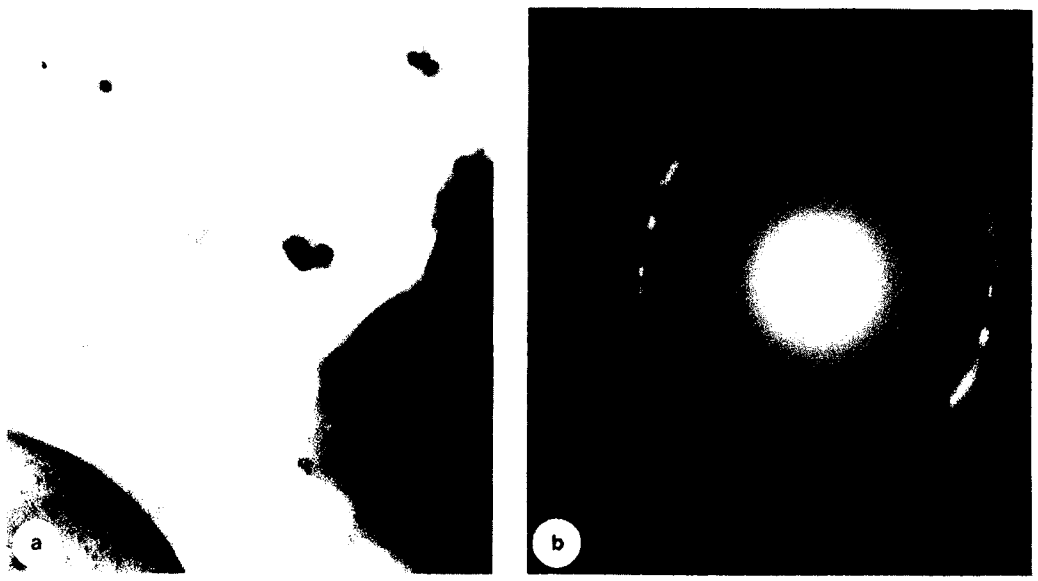

FIG. 2. (a) Transmission electron micrograph of $Pd_{80}Si_{20}$ unthinned sample as quenched, showing small crystallites immersed in an amorphous matrix, 24,000×. (b) Diffraction pattern of $Pd_{80}Si_{20}$ sample in (a). The glassy band is very faint.

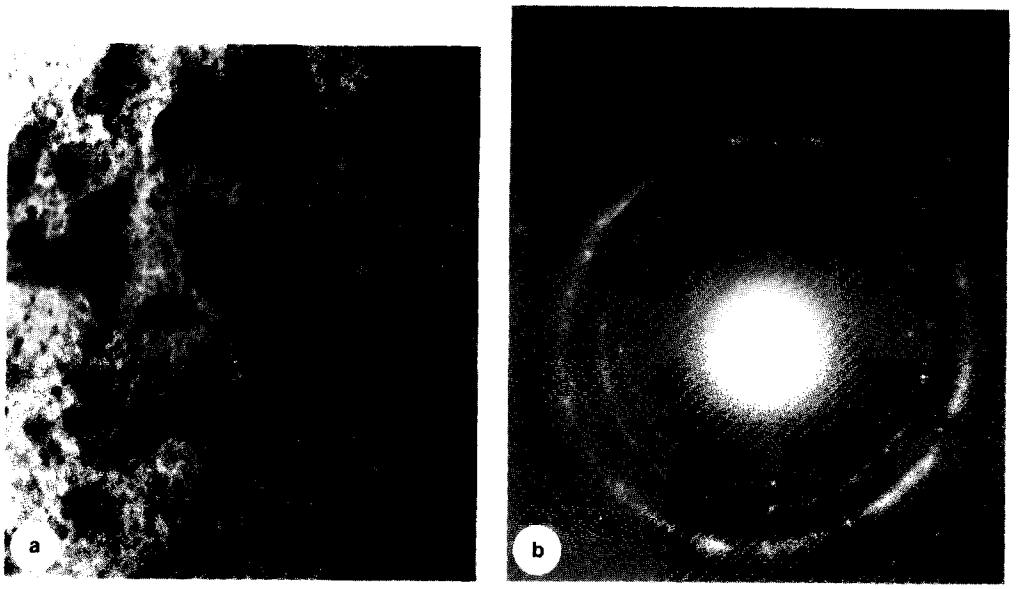

FIG. 3. (a) Transmission electron micrograph of $Pd_{80}Si_{20}$ sample heated to 630°C in vacuum, showing a dense population of 500-Å crystallites, 240,000×. (b) The diffraction pattern of $Pd_{80}Si_{20}$ sample from (a).

tially glassy structure. The apertures used in the HVEM environmental cell prevent viewing diffraction at higher scattering angles. The same diffraction pattern and image were obtained at each isothermal vacuum aging step up to 600°C. At 630°C the diffraction lines attributed to Pd_9Si_2 and Pd_3Si appeared in place of the glassy bands. The emerging diffraction pattern of $Pd_{80}Si_{20}$ sample at 630°C is shown in Fig. 3b. The corresponding image shown in Fig. 3a shows a dense population of 500-Å crystallites. The measured *d* spacings and estimated relative intensities of the observed diffraction lines are shown in Table 1. Shown for comparison in Table 1 are the results of Duhaj *et al.* (*9*) and Masumoto and Maddin (*10*) for vacuum aging of $Pd_{80}Si_{20}$.

Two of these lines match (221) and (404) lines of Pd_9Si_2, according to crystallographic data provided by Nylund (*8*). Duhaj (*9*) also reported (221) and (404) Pd_9Si_2 lines in TEM diffraction studies of crystallized $Pd_{80}Si_{20}$. Except for the first line, with corresponding lattice distance 2.80 Å, all other lines have corresponding *d* spacings in good agreement with data provided by Masumoto and Maddin (*10*) for MS II and Pd_3Si. MS II is a metastable phase formed from $Pd_{80}Si_{20}$ glass with an unknown crystal structure (*10*). However, the comparison of intensities for our two strongest observed lines in vacuum, 2.50 and 2.10 Å, gives good agreement only with Masumoto and Maddin's data for Pd_3Si.

Three other lines, 1.63, 1.43, and 1.36 Å, cannot be compared with the Masumoto and Maddin data for Pd_3Si, because in that work the smallest lattice distance is 1.80 Å. Line 1.63 Å can be only attributed to MS II. The intensity comparison also gives a good agreement.

Lines 1.43 and 1.36 Å are also in good agreement with MS II lines in terms of both lattice distance and relative intensity. They can also match Pd_9Si_2 (404) and Pd_9Si (004) from Duhaj's work.

B. Cyclohexane Aging

The same heating procedures shown in Fig. 1 was repeated with another unthinned

TABLE I

Analyzed Results of Electron Diffraction Patterns Obtained by Stepwise Heating of $Pd_{80}Si_{20}$ Glass *in Situ* in Vaccum and Cyclohexane

Line number	HVEM results				Duhaj *et al.*[a]		Masumoto and Maddin					
	Vacuum		Cyclohexane		Phase (*hkl*)	*d* (Å)	Phase	*d* (Å)	Intensity I_{obs}	Phase (*hkl*)	*d* (Å)	Intensity, I_{obs}
	Lattice distance, *d* (Å)	Intensity, I_{obs}	Lattice distance, *d* (Å)	Intensity I_{obs}								
1	2.80	m	—	—	Pd_9Si_2(221)	2.78	—	—	—	—	—	—
2	—	—	2.73	m	—	—	MS II	2.689	w	Pd_3Si(121)	2.701	m
3	2.50	s	2.50	vs	Pd_3Si(012)	2.48	MS II	2.516	w	Pd_3Si(201)	2.510	m
4	—	—	2.27	s	—	—	MS II	2.278	s	Pd_3Si(031)	2.270	s
5	2.10	vs	—	—	—	—	MS II	2.098	m	Pd_3Si(221)	2.098	s
6	—	—	2.04	vw	—	—	MS II	2.017	w	Pd_3SI(122)	2.014	m
7	—	—	1.82	w	—	—	MS II	1.800	w	Pd_3Si(301)	1.800	w
8	1.63	vw	1.64	w	—	—	MS II	1.630	vw	—	—	
9	—	—	1.56	w	—	—	MS II	1.527	vw	—	—	
10	—	—	1.49	w	—	—	MS II	1.483	vw	—	—	
11	1.43	w	1.42	w	Pd_9Si_2(404)	1.43	MS II	1.452	vw	—	—	
12	1.36	m	1.36	m	Pd_3Si(004)	1.33	MS II	1.375	m	—	—	
13	—	—	1.25	vw	—	—	MS II	1.244	vw	—	—	

Note. Shown for comparison are the results of Duhaj *et al.* (*9*) and Masumoto and Maddin (*10*).

[a] Corresponding lattice distances calculated from crystallographic data of Nylund (*8*) for orthorhombic Pd_9Si_2, $a = 7.418$ Å, $b = 9.396$ Å, $c = 9.048$ Å; and from Aronsson (*12*) for orthorhombic Pd_3Si, $a = 4.735$ Å, $b = 7.555$ Å, $c = 5.260$ Å.

$Pd_{80}Si_{20}$ flake in the presence of 20 Torr of cyclohexane in the HVEM environmental cell. The room temperature diffraction pattern of this second sample was identical to the pattern shown in Fig. 2b for the vacuum aged sample of $Pd_{80}Si_{20}$. During aging at 150°C the image darkened, apparently due to the adsorption of cyclohexane on the metallic glass surface. Below 405°C no crystalline diffraction lines emerged. At 405°C diffraction lines emerged as shown in Fig. 4b; the image showed a dense population of 1000-Å crystallites (Fig. 4a).

The measured *d* spacings and estimated relative intensities of the observed diffraction lines from cyclohexane aging are also shown in Table I for comparison to the vacuum aging results. The relative intensities of the two strongest lines, 2.40 and 2.27 Å, are in good agreement only with Pd_3Si (*10*). The measured *d* spacings for the first five lines match both Pd_3Si and MS II (*10*). In the presence of cyclohexane seven new lines appeared, all of which are in the *d*-spacing range for measured diffraction lines in the vacuum aged sample. Two lines at 2.80 and 2.10 Å, which appeared at medium and very strong intensities during vacuum aging, did not appear during aging in cyclohexane. Three of the new lines are in good agreement with data for Pd_3Si (*10*) in terms of both *d* spacings and relative intensity. Four of them are in good agreement with MS II (*10*) in terms of both relative intensity and *d* spacings.

DISCUSSION

The environmental cell and the hot stage of the HVEM made possible the study of the crystallization of $Pd_{80}Si_{20}$ glass *in situ* both in vacuum and under conditions simulating a reaction. The crystallization temperature was found to be 630°C in vacuum. The transformation of $Pd_{80}Si_{20}$ to Pd_3Si was reported before in vacuum at 500°C (*9*). The presence of cyclohexane had a significant effect on the crystallization of $Pd_{80}Si_{20}$ glass sample. The crystallization temperature was lowered by about 200°C (Fig. 1). This kind of adsorption effect on the bulk crystallization of a metallic glass was reported by Masumoto and co-workers (*3*),

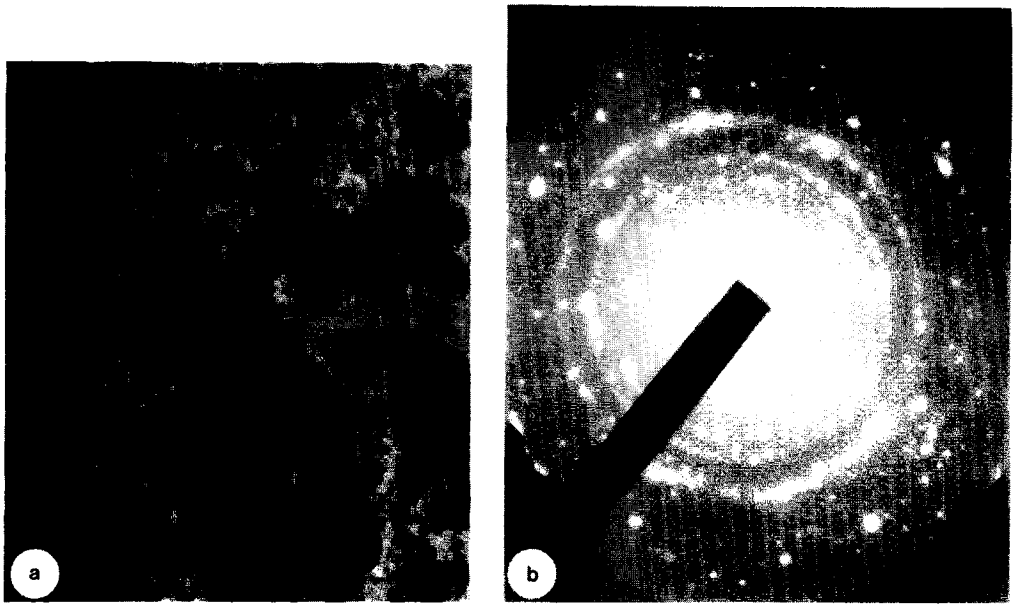

FIG. 4. (a) Transmission electron micrograph of the unthinned $Pd_{80}Si_{20}$ sample heated to 405°C in the presence of cyclohexane, showing a dense population of 1000-Å crystallites, 24,000×. (b) Diffraction pattern of the $Pd_{80}Si_{20}$ sample from (a).

who reported a 132°C lowering of the crystallization temperature of $Fe_{80}B_{20}$ glass during the Fischer–Tropsch reaction.

The other effect of cyclohexane adsorption was to alter the path of the phase transformation of the $Pd_{80}Si_{20}$ metallic glass itself. As can be seen in Table 1, four diffraction lines are common to both aging atmospheres. Three out of these four lines index well to Pd_3Si. Two of the lines in the vacuum aging pattern do not appear in the cyclohexane patterns 2.10 Å, associated with Pd_3Si, and 2.80 Å, associated with Pd_9Si_2. Thus, it appears that the Pd_3Si phase is common to both atmospheres, but the Pd_9Si_2 does not appear in cyclohexane. Since all seven new lines in the cyclohexane pattern can be associated with MS II and Pd_3Si, the cyclohexane aging atmosphere apparently induces the crystallization of a MS II second phase with Pd_3Si, whereas the vacuum aging induces a Pd_3Si and Pd_9Si_2 two phase structure. Although the above interpretation of the crystal structures appearing on aging is not without ambiguity, the strong differences between the two diffraction patterns clearly indicate a different crystallization path for $Pd_{80}Si_{20}$ glass in vacuum as opposed to cyclohexane.

The change of the crystallization path for $Pd_{80}Si_{20}$ glass in the presence of cyclohexane differs from the effect of adsorbed reactants observed by Masumoto and co-workers, where the reaction conditions lowered the crystallization temperature of $Fe_{80}B_{20}$ glass, but did not affect the structure of the transformed glass.

The darkening of the TEM image after exposure to cyclohexane indicates at least physiosorption and probably chemisorption of the cyclohexane occurred. Such chemisorption induced glass crystallization could be the analog of chemisorption induced surface segregation as observed by Sachtler and co-workers (*11*).

The authors feel that the enhancement of crystallization kinetics by the presence of chemisorbed cyclohexane may be evidence for a sort of catalysis in reverse. Just as the

reactant molecules are faced with an activation energy barrier, the metastable glassy structure, which comprises the $Pd_{80}Si_{20}$ alloy catalyst, is attempting to crystallize by surmounting the activation barrier for crystallization. The usual case for the rate limiting step in phase transformations of alloys in the solid state is diffusion of solute. Thus, it appears that the chemisorbed cyclohexane weakens the bonds between surface palladium and silicon atoms and allows surface diffusion and the subsequent crystallization at a higher rate than the vacuum case.

CONCLUSIONS

The adsorption of cyclohexane has a strong effect on the crystallization kinetics of the metastable $Pd_{80}Si_{20}$ metallic glass. The crystallization temperature was lowered by 200°C as compared to vacuum conditions. In addition, the path of the crystallization was altered from vacuum conditions, which apparently generate a mixture of Pd_3Si and Pd_9Si_2, to cyclohexane conditions, which generate a mixture of Pd_3Si and MS II.

ACKNOWLEDGMENTS

The authors are grateful to the staff of the HVEM facility at Argonne National Laboratory. This work was sponsored by the Materials Science Division, OBES, U.S. DOE.

REFERENCES

1. Smith, G. V., Zahraa, O., Molnar, A., Kahn, M. M., Richter, B., and Brower, W. E., *J. Catal.* **83,** 238 (1983).
2. Brower, W. E., Jr., Matyjaszczyk, M. S., Petit, T. L., and Smith, G. V., *Nature (London)* **301,** 497 (1983).
3. Yokoyama, A., Komiyama, H., Inoue, H., Masumoto, T., and Kimura, H. M., *J. Catal.* **68,** 355 (1981).
4. Alp, E. E., Saporoshenko, and Brower, W. E., Jr., *in* "Proceedings, Conference of Rapidly Quenched Metals, Würtzburg, West Germany, 1984."
5. Wagner, C. J., *Adv. X-Ray Anal.* **12,** 50 (1969).
6. Duwez, P., *Trans Amer. Soc. Met.* **60,** 605 (1967).
7. Scott, M. G., *in* "Amorphous Metallic Alloys" (F. E. Loborsky, Ed.). Butterworths, London, 1983.
8. Nylund, A., *Acta Chem. Scand.* **20,** 2381 (1966).
9. Duhaj, P., Sladek, V., and Mrafko, P., *J. Non-Cryst. Solids* **13,** 341 (1973).
10. Masumoto, T., and Maddin, R., *Acta Metall.* **19,** 725 (1971).
11. Bouwman, R., Lippits, G. H. M., and Sachtler, W. M. H., *J. Catal.* **25,** 350 (1972).
12. Aronsson, B., *Acta Chem. Scand.* **20,** 2381 (1966).